Solar Physics
DOI: 10.1007/•••••-•••-•••-••••-•

# Brightness temperature of radio zebras and wave energy densities in their sources

**L.V. Yasnov**[1], **J. Benáček**[2], **M. Karlický**[3]

Received ; accepted

© Springer ••••

**Abstract** We estimated the brightness temperature of radio zebras (zebra pattern – ZP), considering that ZPs are generated in the loops having in their cross-section the exponential density profile. We took into account that when in plasma there is the source emitting in all directions then in an escape process from the plasma the emission obtains directional character nearly perpendicular to the constant density profile. Owing to a high directivity of the plasma emission (for the emission on frequencies close to the plasma frequency) the region from which the emission escapes can be very small. We estimated the brightness temperature of three observed ZPs for two values of the density height scale (1 and 0.21 Mm) and two values of the loop width (1 and 2 arcsec). In all cases high brightness temperatures were obtained. For the higher value of the the density height scale the brightness temperature was estimated as $1.1 \times 10^{15}$ – $1.3 \times 10^{17}$, and for the lower value as $4.7 \times 10^{13}$ – $5.6 \times 10^{15}$. These temperatures show that the observation probability of the burst with ZP, that is generated in the transition region with a steep gradient of the plasma density, is significantly higher than for the burst generated in the region with smoother changes of the plasma density. We also computed the saturation energy density of the upper-hybrid waves (which according to the double plasma resonance model are generated in the zebra source) using a 3-D particle-in-cell model with the loss-cone type of distribution of hot electrons. We found that this saturated energy is proportional to the ratio of hot electron and background plasma densities. Thus, comparing the growth rate and collisional damping of the upper-hybrid waves we estimated minimal densities of hot electrons as well as minimal value of the saturation energy density of the upper-hybrid waves. Finally, we compared the computed energy density of the upper-hybrid waves with the energy density of the electromagnetic waves in the zebra source and thus estimated the efficiency of the wave transformation.

[1] St.-Petersburg State University, St.-Petersburg, 198504, Russia (e-mail: l.yasnov@spbu.ru)
[2] Department of Theoretical Physics and Astrophysics, Masaryk University, Kotlářská 2, CZ – 611 37 Brno, Czech Republic (e-mail: jbenacek@physics.muni.cz)
[3] Astronomical Institute, Academy of Sciences of the Czech Republic, 251 65 Ondřejov, Czech Republic (e-mail: karlicky@asu.cas.cz)

arXiv:1702.01278v1 [astro-ph.SR] 4 Feb 2017

**Keywords:** Solar corona, Flares, Radio bursts

## 1. Introduction

Fine structures of solar radio bursts are very important for understanding of flare energy-release processes and diagnostics of the flare plasma. Among various fine structures the most intriguing one is the zebra structure (ZP - zebra pattern) occurring in type IV radio bursts. In radio spectra it looks as several parallel stripes distributed equidistantly in frequencies, see examples in the following. Usually the number of such zebra stripes in ZP is large ($> 5-8$, sometimes even exceeding 20).

Up to now there are still questions about the generation mechanism of these ZPs. Among many proposed models (Zheleznyakov and Zlotnik, 1975; LaBelle *et al.*, 2003; Kuznetsov and Tsap, 2007; Bárta and Karlický, 2006; Tan, 2010; Karlický, 2013), the most commonly accepted model is that based on the double plasma resonance (DPR) (Zlotnik, 2013; Karlický and Yasnov, 2015). Based on this model most of observed characteristics of ZPs were explained: the frequency range, polarization, amount of stripes and their frequencies, their high-frequency limit and their time changes.

However, up to now in literature there are only few estimations of the ZP brightness temperature that is important for further specification of the generation mechanism of ZPs. For example, Chernov *et al.* (1994) estimated the brightness temperature of metric ZPs to be $10^{10}$ K with the source size constrained by the Nancay Radioheliograph.

Further estimation of the ZP brightness temperature ($T_b = 10^{13}$ K) can be found in the paper by Chernov, Yan, and Fu (2003) where the ZP consisted spiky superfine structures, see also Chernov (2006). On the other hand, Chernov (2006) states that the metric ZP radio sources occupy a noticeable part of the background continuum source or even the entire active region. The half width of one source of the metric ZP was about 1.9 arcmin, which gives the brightness temperature of $10^{10}$ K.

Using the Siberian Solar Radio Telescope (SSRT) Altyntsev *et al.* (2005) observed the ZP burst at $\approx 5.7$ GHz (the highest frequency ever reported for ZP emission), which yielded a lower limit of $T_b \approx 2 \times 10^7$ K.

In the paper by Chen *et al.* (2011) the lower limit for the decimetric ZP brightness temperature was estimated as $1.6 \times 10^9$ K. Finally, Tan *et al.* (2014) estimated the brightness temperature of the decimetric ZP as $T_b \approx 2 \times 10^{11}$.

In the present paper we estimate the brightness temperature of ZP considering that ZP is generated in the loop having in its cross-section the exponential density profile. In this case, the ZP source size and brightness temperature depend on the loop cross-section size. Furthermore, using a 3-D particle-in-cell model with the loss-cone type of distribution of hot electrons we compute the energy density of the upper-hybrid waves. Then this energy density is compared with that of the electromagnetic waves and thus the efficiency of the wave transformation (which is not well known) is estimated.

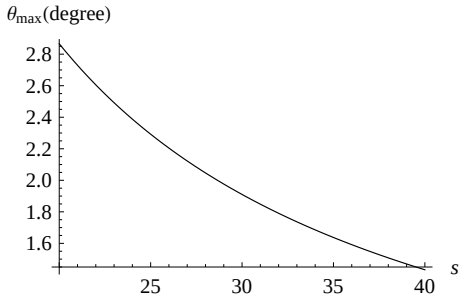


**Figure 1.** Maximum escape angle of the plasma emission in conditions of the double-plasma resonance vs. the gyro-harmonic number $s$.

## 2. Sizes of the zebra source

If in plasma there is a source emitting in all directions then the emission during its escape process obtains directional character. The range of angles $\leq \Theta_{max}$, in which the emission escapes, can be expressed as (Zheleznyakov, 1997)

$$\Theta_{max} = \text{arcsec}\left(\frac{\omega}{\omega_{\rm L}}\right), \tag{1}$$

where $\omega_{\rm L}$ is the plasma frequency in the source and $\omega$ is the emission frequency. In conditions of the double plasma resonance the ratio of these frequencies is (Karlický and Yasnov, 2015)

$$\frac{\omega}{\omega_{\rm L}} = \frac{s}{\sqrt{s^2-1}}, \tag{2}$$

where $s$ is the gyro-harmonic number.

In Figure 1 the maximum escape angle of the plasma emission for the double-plasma resonance in dependance on the gyro-harmonic number $s$ is shown.

Owing to a high directivity of the plasma emission (for the emission on frequencies close to the plasma frequency) a region from which the emission escapes can be very small. It is connected with the fact that the emission region in the flare loop on a fixed frequency is not flat due to a density inhomogeneity across the loop (the maximum density is expected at the loop axis). It has a convex form and thus the emission with a high directivity (having the maximum in the direction perpendicular to a constant density layer) can reach an observer only from a limited region.

In the paper by Watko and Klimchuk (2000) it was shown that the width of loops close to their footpoints, where the decimetric bursts are generated, is about 0.5 arcsec (0.36 Mm), and the typical width of higher loops is about 1 arcsec. Note that the decimetric ZPs are generated in loops at low heights (about 3 Mm) (Karlický and Yasnov, 2015;Yasnov, Karlický, and Stupishin, 2016). The width of some loops can be even smaller. For example, Peter *et al.* (2013) found tiny 1.5MK loop-like structures that they interpret as miniature coronal loops. Their coronal segments above the chromosphere have a length of only about

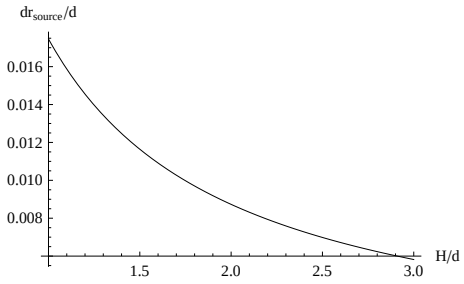


**Figure 2.** The source extent $\Delta r_{source}/d$ in dependance on $H/d$ for the emission nearly perpendicular (for the maximum escape angle = 2 degree) to the constant density profile.

1Mm and a thickness of less than 200 km. Moreover, Peter and Bingert (2012) showed that in a 3-D self-consistent magnetohydrodynamic model of the solar corona the loop width remains constant with height and profiles of intensities along the loop radius correspond to gaussian ones. The gaussian profile along the loop radius was considered also in the paper by Chernov *et al.* (1994). Kuznetsov and Kontar (2015) assumed the gaussian function ($\exp(-r^2/a^2)$, where $r$ is the loop radius and $a = 1$ arcsec) describing the electron distribution in the flare loop.

Therefore, in agreement with the above mentioned papers, we assume that the density inside the magnetic loop at specific height $h_0$ has the exponential form

$$n_{\rm e}(x,z) = n_{\rm em}(h_0)\exp\left(-\frac{r^2}{d^2}\right), \tag{3}$$

where $n_{\rm em}$ is the density at the loop axis, $d$ is the parameter expressing the loop width, and $r$ is the radius across the loop. Moreover, the density in the loop decreases with the height as $\sim \exp(-(h-h_0)/H$, where $h$ is the height in the solar atmosphere and H is the height scale. Thus, the density inside the loop can be expressed as

$$n_{\rm e}(x,z,h) = n_{\rm em}(h_0)\exp\left(-\frac{r^2}{d^2}\right)\exp\left(-\frac{h-h_0}{H}\right). \tag{4}$$

Now, let us calculate the form of the layer with the constant plasma density. For the height, where this layer is located, we can write

$$C = n_{\rm em}(h_0)\exp\left(-\frac{r^2}{d^2}\right)\exp\left(-\frac{h-h_0}{H}\right), \tag{5}$$

$$h(r) = h_0 - H\frac{r^2}{d^2} + H\ln\left(\frac{n_{\rm em}(h_0)}{C}\right), \tag{6}$$

where $C$ is the constant.

In the loop with the constant magnetic field, from the pressure equilibrium and density variation follow that the temperature varies and thus also the height-scale. However, for simplification in further calculations, we assume that the height-scale $H$ inside the loop is constant.

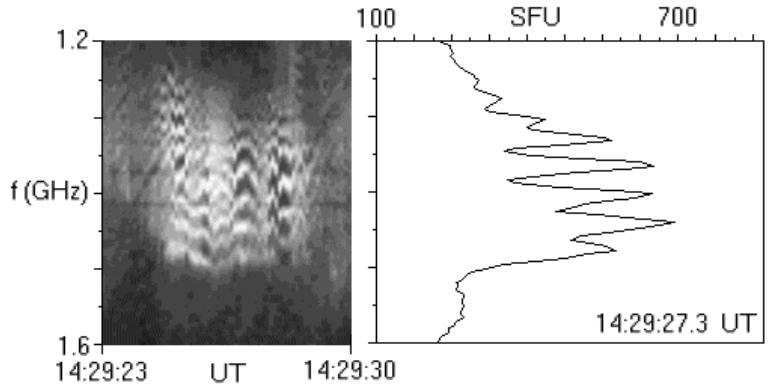


**Figure 3.** Left panel: An example of the zebra pattern observed by Ondřejov radiospectrograph during the 2 May 1998 solar flare. Right panel: The radio flux profile along the frequency at 14:29:27.3 UT.

Then the derivation of $dh/dr$ is

$$\frac{dh}{dr} = -\frac{2Hr}{d^2}. \tag{7}$$

Using this derivation, the extent of the emission region for which the emission direction is nearly perpendicular to the constant density profile can be estimated as

$$\Delta r_{\rm source} = \frac{d^2 \tan(\Theta_{max})}{2H}, \tag{8}$$

where $\Theta_{max}$ is the maximum escape angle of the plasma emission according to the relation 1 (Figure 1). Note that the extent is independent of $r$. An example of the dependance of $\Delta r_{\rm source}/d$ on $H/d$ for $\Theta_{max} = 2$ degrees is shown in Figure 2.

The emission source is also extended in height. This dimension can be estimated as $h_s = \mathrm{H(df/f)}$, where df is the bandwidth of the zebra stripe and f the zebra stripe frequency.

## 3. Estimations of the brightness temperature of zebra structures

Now, let us estimate the brightness temperature of some observed ZPs. For this purpose we selected three ZPs observed by the Ondřejov radiospectrograph (Jiricka *et al.*, 1993), see Figures 3, 4, and 5.

The brightness temperature can be expresses as (Zaitsev and Stepanov, 1983)

$$T_b = \frac{S}{7 \times 10^{-11}} \frac{1}{f_{\rm GHz}^2 L_8^2}, \tag{9}$$

where $S$ is the radio flux in SFU, $f_{\rm GHz}$ is the frequency in GHz, and $L_8$ ($= 2\Delta r_{\rm source}$) is the dimension of the emission region in unit $10^8$ cm.

Thus to compute the brightness temperature, we need to determine the source size $\Delta r_{\rm source}$. First, using the method presented by Karlický and Yasnov (2015)

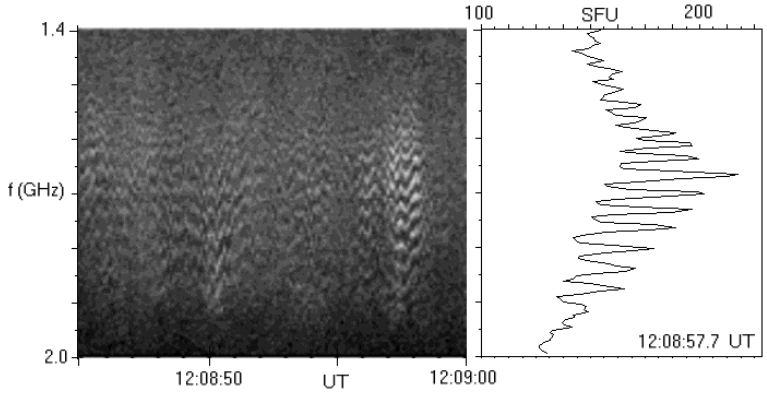


**Figure 4.** Left panel: An example of the zebra pattern observed by Ondřejov radiospectrograph during the 14 February 1999 solar flare. Right panel: The radio flux profile along the frequency at 12:08:57.7 UT.

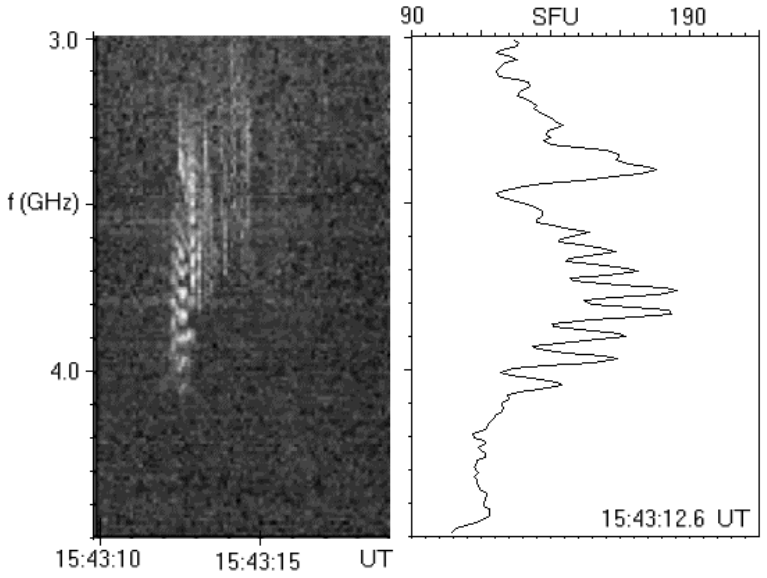


**Figure 5.** Left panel: An example of the zebra pattern observed by Ondřejov radiospectrograph during the 6 June 2000 solar flare. Right panel: The radio flux profile along the frequency at 15:43:12.6 UT.

we determined the gyro-harmonic numbers $s_1$ for the observed zebras. Knowing $s_1$ (see Table 1) and considering the height scale as H (m) = 50 T (K) (Priest, 2014) for the temperature T = $2 \times 10^4$ K, we calculated the source size of the observed zebras for two values of $2d$ (1 and 2 arcsec). All computed parameters of the zebra sources together with the brightness temperatures are shown in Table 1.

However, in the region with a rapid change of the plasma temperature, the height scale can be shorter. Therefore, let us estimate the brightness temperature using the model by Selhorst, Silva-Válio, and Costa (2008). For typical densities

**Table 1.** ZP source parameters. $S$ is the radio flux in SFU units $s_1$ means the gyro-number of the stripe with the lowest frequency.

| | ZP 2 May 1998 | ZP 14 February 1999 | ZP 6 June 2000 |
|---|---|---|---|
| Event location | S15W15 | N16E09 | N23E15 |
| $S$(SFU) | 650 | 170 | 210 |
| $f_{\rm GHz}$ | 1.45 | 1.67 | 3.78 |
| $s_1$ | 21 | 32 | 34 |
| $\Theta_{max}$ | 2.70 | 1.79 | 1.68 |
| $L_8$ (2 d=1 arcsec) | 0.0059 | 0.0038 | 0.0035 |
| $L_8$ (2 d=2 arcsec) | 0.023 | 0.015 | 0.014 |
| $T_b$ (2 d =1 arcsec) | $13 \times 10^{16}$ K | $6 \times 10^{16}$ K | $1.7 \times 10^{16}$ K |
| $T_b$ (2 d =2 arcsec) | $0.83 \times 10^{16}$ K | $0.39 \times 10^{16}$ K | $0.11 \times 10^{16}$ K |
| Source height (km) | 28 | 14.7 | 12.5 |

**Table 2.** ZP source parameters for H=0.21Mm.

| | ZP 2 May 1998 | ZP 14 February 1999 | ZP 6 June 2000 |
|---|---|---|---|
| $L_8$ (2 d=1 arcsec) | 0.028 | 0.018 | 0.017 |
| $L_8$ (2 d=2 arcsec) | 0.11 | 0.070 | 0.067 |
| $T_b$ (2 d =1 arcsec) | $5.6 \times 10^{15}$ K | $2.7 \times 10^{15}$ K | $0.73 \times 10^{15}$ K |
| $T_b$ (2 d =2 arcsec) | $0.36 \times 10^{15}$ K | $0.18 \times 10^{15}$ K | $0.047 \times 10^{15}$ K |

in ZP sources $5.0\times\ 10^{\ 9}$ cm $^{-3}$ - $3.6\times\ 10^{10}$ cm$^{-3}$ the model gives heights in the solar atmosphere between 2.84 Mm and 3.27 Mm. Thus, the height scale is H = 0.21Mm, which is almost 5 times shorter than that according to the above used Priest's formula. For such a height scale the ZP source parameters are given in the Table 2.

## 4. Energy densities of electromagnetic and upper-hybrid waves in the ZP source

Let us consider the zebra observed during the 2 May 1998 event. Knowing the ZP radio flux (650 SFU) and the zebra line frequency width (40 MHz), and computing the ratio of the emission area at 1 AU (corresponding to the emission directivity angle (2.7 degree for s=21, see Figure 1)), and ZP source area ($L_8 \times L_8$ for four cases according to Tables 1 and 2), the energy density of electromagnetic waves in the ZP source are calculated, see the second column in Table 3.

In the double plasma resonance (DPR) model of ZPs, it is assumed that in the ZP source there are hot electrons with a loss-cone type distribution together with much denser background plasma. The distribution is unstable and generate

the upper-hybrid waves which after their transformation produce the observed ZPs.

Therefore, besides the estimation of the energy density of electromagnetic waves, it is highly desirable to estimate the energy density of the upper-hybrid waves in the ZP source. For this purpose we use a 3-D particle-in-cell (PIC) relativistic code (Buneman and Storey, 1985, Matsumoto and Omura, 1993, Karlický and Bárta, 2008). Although this code is very useful for such computations, it has own limits. Therefore some parameters of ZP from 2 May 1998 cannot be fulfilled in the following PIC computations. For example, there is a problem to make computations with high gyro-harmonic numbers (s > 6 in our case).

The size of the model is $L_x \times L_y \times L_z = \lambda\Delta \times \lambda\Delta \times 32\Delta$, where $\Delta$ is grid size and $\lambda = 12$ is the wave length of the upper-hybrid wave in resonance in normalized units. We chose the model containing only one wave length of the upper-hybrid wave to simplify the processing and decrease computing time. The model time step is $dt = 1$, plasma electron frequency $\omega_{pe}dt = 0.05$, initial magnetic field is in $z$ direction, electron cyclotron frequency is $\omega_{ce} = 0.169\ \omega_{pe}$ corresponding to the harmonic number $s = 6$. In the model we use two groups of electrons: cold background electrons with the thermal velocity $v_{\rm tb} = 0.03$ c (c is the light speed), corresponding to temperature 5.35 MK, and hot electrons with the DGH (Dory, Guest, and Harris, 1965) distribution function for $j = 1$ in the form

$$f = \frac{u_\perp^2}{2(2\pi)^{3/2} v_{\rm t}^5} \exp\left(-\frac{u_\perp^2 + u_\parallel^2}{2v_{\rm t}^2}\right), \tag{10}$$

where $u_\perp = p_\perp/m_{\rm e}$ and $u_\parallel = p_\parallel/m_{\rm e}$ are electron velocities and $p_\perp$ and $p_\parallel$ are components of the electron momentum perpendicular and parallel to the magnetic field, $m_e$ is the electron mass, and $v_{\rm t} = 0.2$ c is the thermal spread in the velocities of hot electrons.

The electron density of cold electrons per cell was taken as $n_{\rm e} = 240$ and the ratio of hot and background plasma electrons electrons as $n_{\rm h}/n_{\rm e} = 1/8$. We also made computations with $n_{\rm h}/n_{\rm e} = 1/16$ and $1/32$ to know the dependence of the saturation energy of the upper-hybrid waves on the density ratio $n_{\rm h}/n_{\rm e}$. The number of protons is the same as electrons and their temperature is the same as that for cold electrons.

Using this PIC code, the time evolution of the electric energy of the upper-hybrid waves $E_{\rm UH}$, generated by hot electrons, is shown in Figure 6. After short beginning phase the electric energy oscillates with the increasing amplitude determined by the growth rate, which is similar as that derived in the paper by Benáček, Karlický, and Yasnov (2017). Then at about $\omega_{pe}t = 270$ the energy is saturated. The saturated energy is about $E_{\rm UH} = 2.5 \times 10^{-3}\ E_{\rm h,kin}$, where $E_{\rm h,kin}$ is the kinetic energy of hot electrons.

As mentioned above we also made computations with $n_{\rm h}/n_{\rm e} = 1/16$ and $1/32$, which together with the case $n_{\rm h}/n_{\rm e} = 1/8$ show that decreasing this ratio the saturation energy proportionally decrease.

Now, for the following estimations, let us derive the minimal value of the parameter $n_{\rm h}/n_{\rm e}$. For this purpose we used the analytical expression for the

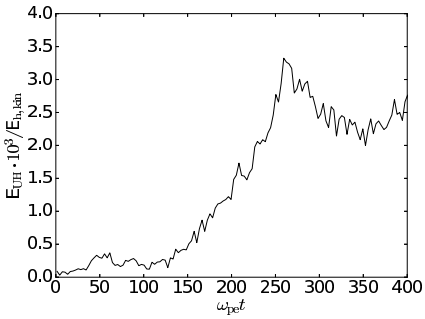


**Figure 6.** Evolution of the ratio of the electric energy of the upper-hybrid waves $E_{\rm UH}$ to the kinetic energy of hot electrons $E_{\rm h,kin}$.

**Table 3.** Energy densities of electromagnetic and upper-hybrid waves in the ZP source for the 2 May 1998 event. $\epsilon = W_{\rm elm}/W_{\rm UH}$ is the parameter expressing the efficiency of transformation of the upper-hybrid waves into electromagnetic ones.

| $L_8$ (Mm) | $W_{\rm elm}$ (J m$^{-3}$) | $W_{\rm UH,min}$ (J m$^{-3}$) | $\epsilon$ |
|---|---|---|---|
| 0.0059 | $3.90\times 10^{-8}$ | $5.41\times 10^{-5}$ | $7.21\times 10^{-4}$ |
| 0.023 | $2.57\times 10^{-9}$ | $5.41\times 10^{-5}$ | $4.75\times 10^{-5}$ |
| 0.028 | $1.73\times 10^{-9}$ | $5.41\times 10^{-5}$ | $3.20\times 10^{-5}$ |
| 0.11 | $1.12\times 10^{-10}$ | $5.41\times 10^{-5}$ | $2.07\times 10^{-6}$ |

growth rate of the upper-hybrid waves as derived by Thejappa (1991)

$$-\gamma_{\rm UH} \approx 4.4\times 10^{-2}\omega_{pe}\frac{n_{\rm h}}{n_{\rm e}}. \tag{11}$$

This growth rate agrees to that in our PIC simulations. To generate the upper-hybrid waves this growth rate needs to be greater than the damping of these waves by collisions

$$\gamma_{\rm c} = 2.75\frac{n_{\rm e}}{T_{\rm e}^{3/2}}\ln\left(10^4 T_{\rm e}^{3/2}/n_{\rm e}^{1/3}\right), \tag{12}$$

where $T_{\rm e}$ is the background plasma temperature. Thus, when we put $\gamma_{\rm UH}$ to be equal to $\gamma_{\rm c}$, then for the mean ZP frequency (1.45 GHz and corresponding plasma density $n_{\rm e} = 2.6\times 10^{16}$ m$^{-3}$) and for $T_{\rm e}$ in ZP source as $2\times 10^4$ K (at bottom part of the transition region), the minimal ratio of $n_{\rm h}/n_{\rm e}$ is $4.93\times 10^{-4}$.

Now, if we take the density of the hot electrons in the ZP source as equal to the minimal density $n_{\rm h} = 2.6\times 10^{16}\times 4.93\times 10^{-4} = 1.28\times 10^{13}$ m$^{-3}$ and utilizing the linear dependance of the saturated energy of the upper-hybrid waves on $n_{\rm h}$, found in the PIC simulations, then the minimal energy density of

the upper-hybrid waves $W_{\mathrm{UH,min}}$ is calculated, see the third column in Table 3. Note that owing to limits of PIC computations these values were obtained for $s = 6$.

However, if we assume that the energy density of the upper-hybrid waves in the ZP source from May 2, 1998 is the same as $W_{\mathrm{UH,min}}$, then we can calculate the parameter, expressing the efficiency of transformation of the upper-hybrid waves into electromagnetic ones, see the last column in Table 3. However, the ratio $n_{\mathrm{h}}/n_{\mathrm{e}}$ in real conditions needs to be greater than its minimal value, therefore $\epsilon$ in real conditions should be lower. On the other hand, values of the parameter $\epsilon$ will be greater if we would consider the absorption of the electromagnetic waves near the ZP source.

## 5. Conclusions

Closeness of the emission frequency of decimetric zebras to the plasma frequency determines a narrow directivity of the ZP emission. For the exponential density profile across the flaring loop, it gives a small area of such an emission and thus high brightness temperatures. We considered two variants of the density dependance vs. height, *i.e.*, two values of the height scale: 1 Mm according to the Priest's formula (Priest, 2014) and 0.21 Mm for the transition region (Selhorst, Silva-Válio, and Costa, 2008) and two values for the loop width (1 and 2 arcsec). In all cases high brightness temperatures were obtained. For the higher value of the the density height scale the brightness temperature was estimated as $1.1 \times 10^{15} - 1.3 \times 10^{17}$, and for the lower value as $4.7 \times 10^{13} - 5.6 \times 10^{15}$. Such high brightness temperatures speak about coherent mechanism of the ZP emission. Note that these brightness temperatures are close to the brightness temperatures of decimetric spikes (Benz, 1986), which indicates that energies of electrons in the both types of the bursts are similar. Because the emission frequency is close to the plasma frequency, the emission absorption can be high and thus the brightness temperature can be even higher.

Observed sizes of ZP sources can be larger than those assumed here because they are enlarged by the scattering of the emission on density fluctuations in the corona (Bastian, 1994).

We found the lower brightness temperature for shorter height scale. It indicates independently on findings presented in the papers by Yasnov and Karlický (2015), Karlický and Yasnov (2015) and Yasnov, Karlický, and Stupishin (2016) that the observational probability of the burst with zebras, which is generated in the transition region with a steep density gradient, is essentially greater than the burst generated in the region with smoother changes of the plasma density. It is given by an enlargement of the visible emission area in the atmosphere with the high density gradient.

Note that sometimes ZPs appear on the radio spectrum of the type IV (continuum) burst in irregular or in quasi-periodic way (in seconds). It can be explained by small irregular or quasi-periodic motion of the flare loop in the case when the ZP source area is sufficiently small. Then the narrow conus of the emission directivity is oriented to an observer and zebra is observed or vice versa.

Numerical simulations with the 3-D particle-in-cell model having hot electrons described by the DGH distribution function show that firstly the energy density of the upper-hybrid waves exponentially grows with the linear growth rate and then it is saturated. The saturated energy is about $E_{\rm UH}= 2.5 \times 10^{-3}\ E_{\rm h,kin}$ for the ratio of cold and hot electrons $n_{\rm h}/n_{\rm e} = 1/8$, where $E_{\rm h,kin}$ is the kinetic energy of hot electrons. Additional computations with $n_{\rm h}/n_{\rm e} = 1/16$ and $1/32$ showed that decreasing $n_{\rm h}/n_{\rm e}$ the saturation energy proportionally decreases. This dependance enabled us to calculate the saturation energy of the upper-hybrid waves for much smaller ratios of $n_{\rm h}/n_{\rm e}$.

The upper-hybrid waves are generated when the growth rate exceeds the damping of these waves by collisions. For the zebra observed during the 2 May 1998 event it is fulfilled if the ratio of hot and cold electrons $n_{\rm h}/n_{\rm e}$ is greater than $4.93 \times 10^{-4}$. This enabled us to compute the minimal energy density of the upper-hybrid waves in ZP source ($W_{\rm UH,min} = 5.41 \times 10^{-5}$ J m$^{-3}$) and the transformation efficiency of the upper-hybrid waves into electromagnetic ones ($\epsilon = 2.07 \times 10^{-6} - 7.21 \times 10^{-4}$).

**Acknowledgements** M. K. acknowledge support from Grants 16-13277S and 17-16447S of the Grant Agency of the Czech Republic. L. V. Y. acknowledge support from Grant 16-02-00254 of the Russian Foundation for Basic Research. Computational resources were provided by the CESNET LM2015042 and the CERIT Scientific Cloud LM2015085, provided under the programme "Projects of Large Research, Development, and Innovations Infrastructures"

## References

Altyntsev, A.T., Kuznetsov, A.A., Meshalkina, N.S., Rudenko, G.V., Yan, Y.: 2005, On the origin of microwave zebra pattern. *Astron. Astrophys.* **431**, 1037 – 1046. doi:10.1051/0004-6361:20048337.

Bárta, M., Karlický, M.: 2006, Interference patterns in solar radio spectra: High-resolution structural analysis of the corona. *Astron. Astrophys.* **450**, 359 – 364. doi:10.1051/0004-6361:20054386.

Bastian, T.S.: 1994, Angular scattering of solar radio emission by coronal turbulence. *Astrophys. J.* **426**, 774 – 781. doi:10.1086/174114.

Benáček, J., Karlický, M., Yasnov, L.: 2017, . *Astron. Astrophys.* **555**, A1. doi:10.1051/0004-6361/201219473.

Benz, A.O.: 1986, Millisecond radio spikes. *Solar Phys.* **104**, 99 – 110. doi:10.1007/BF00159950.

Buneman, O., Storey, L.R.O.: 1985, Simulations of fusion plasmas by A 3-D, E-M particle code. Technical report.

Chen, B., Bastian, T.S., Gary, D.E., Jing, J.: 2011, Spatially and spectrally resolved observations of a zebra Pattern in a solar decimetric radio burst. *Astrophys. J.* **736**, 64. doi:10.1088/0004-637X/736/1/64.

Chernov, G.P.: 2006, Solar Radio Bursts with Drifting Stripes in Emission and Absorption. *Space Sci. Rev.* **127**, 195 – 326. doi:10.1007/s11214-006-9141-7.

Chernov, G.P., Yan, Y.H., Fu, Q.J.: 2003, A superfine structure in solar microwave bursts. *Astron. Astrophys.* **406**, 1071 – 1081. doi:10.1051/0004-6361:20030779.

Chernov, G.P., Klein, K.L., Zlobec, P., Aurass, H.: 1994, Fine structure in a metric type 4 burst: Multi-site spectrographic, polarimetric, and heliographic observations. *Solar Phys.* **155**, 373 – 390. doi:10.1007/BF00680601.

Dory, R.A., Guest, G.E., Harris, E.G.: 1965, Unstable Electrostatic Plasma Waves Propagating Perpendicular to a Magnetic Field. *Physical Review Letters* **14**, 131 – 133. doi:10.1103/PhysRevLett.14.131.

Jiricka, K., Karlicky, M., Kepka, O., Tlamicha, A.: 1993, Fast drift burst observations with the new Ondrejov radiospectrograph. *Solar Phys.* **147**, 203 – 206. doi:10.1007/BF00675495.

Karlický, M.: 2013, Radio continua modulated by waves: Zebra patterns in solar and pulsar radio spectra? *Astron. Astrophys.* **552**, A90. doi:10.1051/0004-6361/201321356.

Karlický, M., Bárta, M.: 2008, Fragmentation of the Current Sheet, Anomalous Resistivity, and Acceleration of Particles. *Solar Phys.* **247**, 335 – 342. doi:10.1007/s11207-008-9115-x.

Karlický, M., Yasnov, L.V.: 2015, Determination of plasma parameters in solar zebra radio sources. *Astron. Astrophys.* **581**, A115. doi:10.1051/0004-6361/201526785.

Kuznetsov, A.A., Kontar, E.P.: 2015, Spatially Resolved Energetic Electron Properties for the 21 May 2004 Flare from Radio Observations and 3D Simulations. *Solar Phys.* **290**, 79 – 93. doi:10.1007/s11207-014-0530-x.

Kuznetsov, A.A., Tsap, Y.T.: 2007, Loss-cone instability and formation of zebra patterns in type IV solar radio bursts. *Solar Phys.* **241**, 127 – 143. doi:10.1007/s11207-006-0351-7.

LaBelle, J., Treumann, R.A., Yoon, P.H., Karlický, M.: 2003, A model of zebra emission in solar type IV radio bursts. *Astrophys. J.* **593**, 1195 – 1207. doi:10.1086/376732.

Matsumoto, H., Omura, Y.: 1993, *Computer space plasma physics: simulation techniques and software,* Terra Scientific Pub. Co, p.305.

Peter, H., Bingert, S.: 2012, Constant cross section of loops in the solar corona. *Astron. Astrophys.* **548**, A1. doi:10.1051/0004-6361/201219473.

Peter, H., Bingert, S., Klimchuk, J.A., de Forest, C., Cirtain, J.W., Golub, L., Winebarger, A.R., Kobayashi, K., Korreck, K.E.: 2013, Structure of solar coronal loops: from miniature to large-scale. *Astron. Astrophys.* **556**, A104. doi:10.1051/0004-6361/201321826.

Priest, E.: 2014, *Magnetohydrodynamics of the Sun,* Cambridge University Press, UK.

Selhorst, C.L., Silva-Válio, A., Costa, J.E.R.: 2008, Solar atmospheric model over a highly polarized 17 GHz active region. *Astron. Astrophys.* **488**, 1079 – 1084. doi:10.1051/0004-6361:20079217.

Tan, B.: 2010, A physical explanation of solar microwave zebra pattern with the current-carrying plasma loop model. *Astrophys. Space Sci.* **325**, 251 – 257. doi:10.1007/s10509-009-0193-5.

Tan, B., Tan, C., Zhang, Y., Huang, J., Mészárosová, H., Karlický, M., Yan, Y.: 2014, A very small and super strong zebra pattern burst at the beginning of a solar flare. *Astrophys. J.* **790**, 151. doi:10.1088/0004-637X/790/2/151.

Thejappa, G.: 1991, A self-consistent model for the storm radio emission from the sun. *Solar Phys.* **132**, 173 – 193. doi:10.1007/BF00159137.

Watko, J.A., Klimchuk, J.A.: 2000, Width Variations along Coronal Loops Observed by TRACE. *Solar Phys.* **193**, 77 – 92. doi:10.1023/A:1005209528612.

Yasnov, L.V., Karlický, M.: 2015, Regions of Generation and Optical Thicknesses of dm-Zebra Lines. *Solar Phys.* **290**, 2001 – 2012. doi:10.1007/s11207-015-0721-0.

Yasnov, L.V., Karlický, M., Stupishin, A.G.: 2016, Physical Conditions in the Source Region of a Zebra Structure. *Solar Phys.* **291**, 2037 – 2047. doi:10.1007/s11207-016-0952-8.

Zaitsev, V.V., Stepanov, A.V.: 1983, The plasma radiation of flare kernels. *Solar Phys.* **88**, 297 – 313. doi:10.1007/BF00196194.

Zheleznyakov, V.V.: 1997, *Radiation in astrophysical plasmas [in Russian]; Original Russian Title — "Izlucheniye v astrofizicheskoy plasme".*

Zheleznyakov, V.V., Zlotnik, E.Y.: 1975, Cyclotron wave instability in the corona and origin of solar radio emission with fine structure. III. Origin of zebra-pattern. *Solar Phys.* **44**, 461 – 470. doi:10.1007/BF00153225.

Zlotnik, E.Y.: 2013, Instability of electrons trapped by the coronal magnetic field and its evidence in the fine structure (zebra pattern) of solar radio spectra. *Solar Phys.* **284**, 579 – 588. doi:10.1007/s11207-012-0151-1.